Telemanipulator for Remote Minimally Invasive Surgery

Requirements for a Light-Weight Robot for Both Open and Laparoscopic Surgery

BY ULRICH HAGN, TOBIAS ORTMAIER, RAINER KONIETSCHKE, BERNHARD KÜBLER, ULRICH SEIBOLD, ANDREAS TOBERGTE, MATHIAS NICKL, STEFAN JÖRG, AND GERD HIRZINGER

In minimally invasive surgery (MIS), the surgeon works with long instruments through small incisions. These small incisions are the main advantage of MIS, leading to several benefits for the patient when compared with open surgery. These benefits include reduced pain and trauma, reduced loss of blood, reduced risk of wound infections, shorter hospital stays, shorter rehabilitation time, and cosmetic advantages. In contrast to open surgery, direct access to the operation field is no longer possible for the surgeon. According to [1], the loss of direct access leads to several drawbacks for the surgeon: 1) Tissue cannot be palpated any more. 2) Because of the relatively high friction in the trocar, the contact forces between instrument and tissue can hardly be sensed. [The trocar is a surgical device, which makes it possible to create incisions in a visceral cavity (i.e. thorax, abdominal cavity) and keeps it open with the aid of a tube.] This is especially the case when the trocar is placed in the narrow intercostal space (i.e., space between the ribs). 3) As the instruments have to be moved around an invariant fulcrum point, intuitive direct hand–eye coordination is lost, and because of the kinematic restrictions, only 4 degrees of freedom (DoF) remain inside the body of the patient. Therefore, the surgeon cannot reach any point in the work space at an arbitrary orientation. This is a main drawback of MIS, which makes complex tasks like knot tying very time consuming and require intensive training [2].

To overcome the aforementioned drawbacks, telesurgery systems are a promising approach (Figure 1). Within these systems, telemanipulators are key components, as they transfer the surgeon's commands into the patient's body. In combination with appropriate display and telepresence technologies, they allow for a high-grade immersion of the surgeon into the remote site, thus regaining virtually direct access to the operation area comparable to open surgery. The following properties of minimally invasive robotic surgery (MIRS) can be realized with appropriate technologies: 1) Manipulation forces can be measured by miniaturized sensors integrated in the instruments (e.g., see [3]). It is to be expected that the surgeon's situational awareness is increased if the contact situation is displayed to the surgeon by suitable man–machine interfaces (MMIs). 2) By means of control algorithms and actuated surgical instruments, the correct

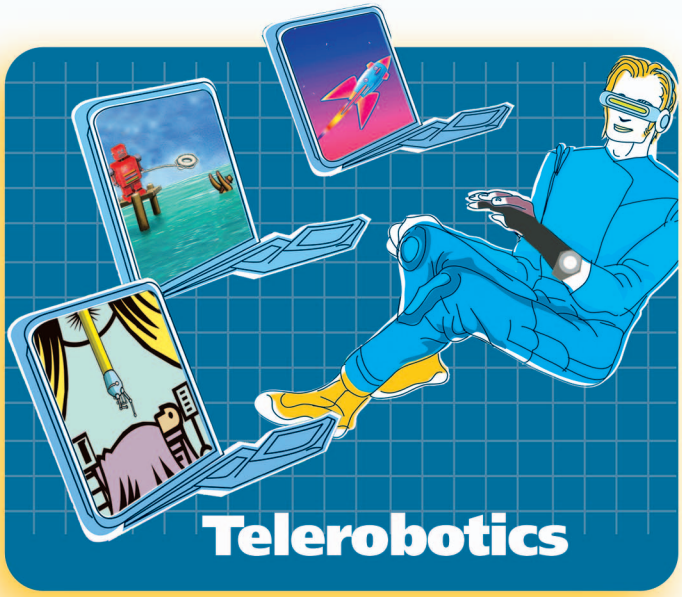

Digital Object Identifier 10.1109/MRA.2008.929925

1070-9932/08/$25.00©2008 IEEE

hand–eye coordination as in the open surgery can be reestablished. 3) More accurate movements are possible, as the surgeon's hand motion can be scaled down before it is transmitted to the robot. Additionally, the surgeon's tremor can be reduced by filters. 4) Furthermore, autonomous functions such as motion compensation can be implemented by MIRS telepresence systems [4], [5]. Thus, surgeons can perform new operation techniques like endoscopic minimally invasive bypass surgery on the beating heart. Intelligent assistance functions help to reduce the operation time (e.g., see [6]) as well as safety functions (e.g., virtual constraints, supervision of manipulation forces) to avoid unintentional damage to the tissue or suturing material. Nevertheless, it has to be noted that the surgical experience reported in [7] leads to the conclusion that, with greater involvement of the surgeon in the surgical workflow, robot-assisted therapies will gain greater acceptance. 5) To become applicable with a wider range of patients, more sophisticated visualization and navigation techniques are required. Additionally, the MMI should allow for an intuitive and ergonomic working style to relieve the surgeon from stress. 6) The possibility to get a third opinion helps to increase the quality of the surgical outcome, as remote experts can be consulted.

In the next section, the requirements for an ideal telemanipulator (i.e., robot and surgical instrument) are derived. Thereafter, an overview on telemanipulators reported in literature is given. The new robot for telepresence surgery developed by German Aerospace Center (DLR) is presented in detail in the "DLR Robot" section. Surgical instruments equipped with miniaturized force-torque sensors and additional DoF at the distal end, also developed by DLR, are described in the "DLR Instruments" section. The last section concludes this article and gives directions for further research.

Requirements for an Ideal Telemanipulator

Robots placed near the patient occupy space in the already crowded operating room (OR) environment. Therefore, these robots have to be as slender and lightweight as possible. Thus, they can be easily mounted or unmounted, and the risk of collisions is reduced. At the same time, the robots have to be as rigid as possible to allow for an accurate and fast positioning of the instrument tip. This imposes high demands on the mechanical structure and the motor dynamics. See also [8] and [9] for a discussion of mechanical properties from a surgical point of view.

Kinematic redundancy of the robots allows for a flexible OR setup, as the robot pose can be changed according to the surgical setup. If the robot is equipped with torque sensors at or near the joints (see e.g., the "Robot Hardware" section), handling forces by the OR staff can be measured. In combination with joint redundancy, this enables an intuitive way to manually reconfigure the robot structure by just pushing and pulling the robot (i.e., haptic interaction), while the tool center point (TCP) remains unchanged. Additionally, this is also a safety feature, as collisions between robot structure and environment can be detected. This is not the case with today's robots, as they are usually equipped only with a TCP mounted force-torque sensor.

The diameter of the surgical instruments that are attached to the robot tool tip has to be as small as possible. This is not only necessary to reduce the incision size (and therefore to reduce trauma) but also to be able to insert the instrument through the narrow intercostal space if used, e.g., in heart surgery. To achieve the full manipulability of 6 DoF inside the patient, at least an additional 2 DoF at the distal end of the instrument are necessary. This is also a prerequisite for intuitive and correct hand–eye coordination to which surgeons are used to in open surgery.

The surgeon is separated from the operation area because of the restricted access described earlier. Consequently, the surgeon is able to neither feel contact forces nor to palpate tissue. An advanced telesurgery system should be able to display this information to the surgeon by appropriate display technologies.

Information about contact forces can be given by augmented reality where contact forces are displayed visually or by directly reflecting them to the user's hand with the aid of haptic input devices. In such a bilateral teleoperating system, the teleoperator (master) and the telemanipulator (slave) are coupled in a closed loop. The design goal is impedance matching of master and slave, so the operator feels virtually interacting directly with the remote environment in the patient. To achieve a transparent system (i.e., good matching of impedance) that provides a good feeling of the manipulated tissue, a tight coupling between the master and the slave is necessary [10]. Lawrence four-channel architecture for bilateral teleoperation is advantageous, where positions and forces are sent from the master to the slave and vice versa. This architecture implies the measurement of positions and forces of the telemanipulator's end effector. This requires locally accurate forward kinematics, since the master kinematics in general differs from the slave and teleoperation is implemented in Cartesian space.

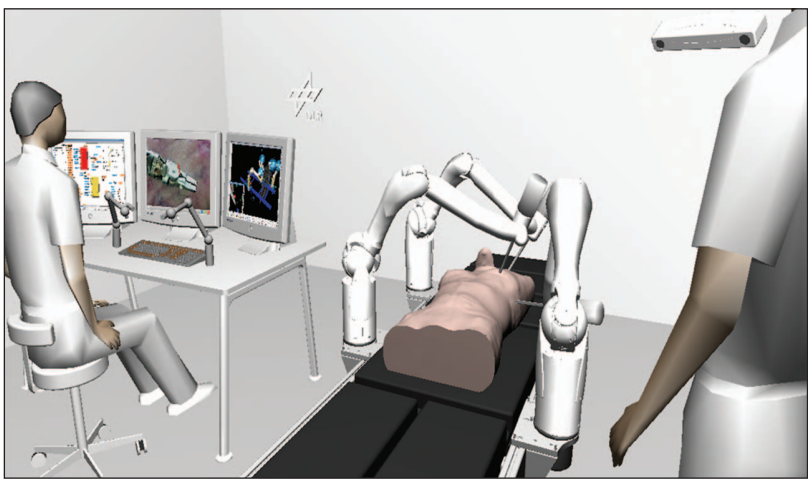

Figure 1. *Schematic illustration of the DLR teleoperated surgery system for MIS. In the front, an assistant surgeon (e.g., for the application and change of instruments) is with the patient. In the background, the surgeon at a master console is directing the instruments.*

Robots placed near the patient occupy space in the already crowded OR environment. Therefore, they have to be as slender and lightweight as possible.

As a prerequisite, a crucial property of the surgical telemanipulator is the ability to measure the contact situation between the instrument and tissue as well as the grasping forces if grippers are used as surgical instruments. Additionally, the measurement of tactile information is still a challenging task, though it is necessary to gain access to invisible structures, e.g., calcification of blood vessels and tumors. To summarize this paragraph, it can be stated that both an appropriate sensor and display technologies are necessary to provide the surgeon with an appropriate degree of immersion into the remote site.

Related Work and State of the Art

Since the early 1990s, more than 35 surgical robotic systems have been developed [11]. In the field of MIRS, especially two commercial systems are to be mentioned: the Zeus system (Computer Motion Inc. [12]) and the da Vinci system (Intuitive Surgical Inc. [13]). The Zeus system is no longer available.

As described earlier, full dexterity inside the patient as well as the decoupled determination of gripping and interaction forces are necessary for an appropriate immersion of the surgeon. Most systems comprising a force-torque sensing modality focus on only one of these states (see the following section).

Under research conditions, a number of prototypic approaches containing kinesthetic feedback could be presented. Hu et al. introduced conventional laparoscopic tools equipped with strain gauge sensors [14]. The sensed forces are displayed by a PHANToM (SensAble Technologies Inc.), a rather widespread kinesthetic device. As this tool is not attached to a robot and the grip is not actuated, the current setup requires two users: one to actuate the surgical instrument and the second one to feel the grasping forces at the PHANToM. As the strain gauge sensors are placed at the proximal end of the instrument, the grasping forces are superposed by friction, and also the measurement of contact forces is not possible at present.

A force-controlled laparoscopic surgical robot without distal force sensing is presented in [15]. A standard force sensor is integrated into a trocar and thus remains outside the patient. This makes it easier to guarantee the required standards of sterilization and requires less effort to miniaturize components. Because of the specific installation of the sensor the measurement is not deteriorated by the friction between the trocar and the instrument. To calculate the contact forces, only gravity compensation is necessary. The robot mainly works in co-manipulation mode, meaning that the surgeon and the robot manipulate the same instrument. Initial experimental in vivo and in vitro results are encouraging.

A similar system is presented in [16]. The authors added force sensors to a modified sterile adapter of the da Vinci system, thus avoiding the integration of tiny sensors into the instrument tip. The goal is to measure interaction forces between the jaw and tissue without deterioration by driving, gravity, and acceleration forces. An overall measurement error of approximately 0.5 N is reported. The heavy adapter (1.2 kg) is moved by the da Vinci arms and does not allow for the measurement of interaction torques.

Previous work at the Institute of Robotics and Mechatronics of the DLR includes prototypes of force sensors with 4 and 6 DoF [17] as well as a prototypic laparoscopic knife equipped with a custom-made miniaturized force-torque sensor close to the instrument tip. An experimental evaluation of this force reflecting the master slave system for laparoscopic surgery is presented in [18]. Twenty-five participants performed robotically assisted artificial artery dissection with and without the force feedback. Cellular rubber was used to model an artificial artery, and the surrounding tissue was replaced with modeling material. The results can be summarized as follows: the dissection speed did not significantly differ if the force feedback was employed or not. In contrast, the injuries of the arteries were drastically reduced when force feedback was available. Similar experiments with and without force feedback are given in [19]. In this article, it was shown that in case of force feedback, significantly less force was applied, whereas speed hardly differed. Therefore, it can be stated that the force feedback leads to a more gentle surgery with less injury to the patient's tissue.

Kobayashi et al. presented a comparably small semiactive robot guiding MIS instruments with two PHANToMs [20]. The system provides full manipulability inside the patient (6 DoF) plus 1 DoF for a functional end (e.g., forceps). All force transmission components to the functional end are link driven and thus are expected to show good proximal force feedback answers because of the high rigidity of the links. However, the presented system is not equipped with force-torque sensors and thus provides no feedback from the operation site to the surgeon.

An interesting approach for the force feedback purely based on control engineering was introduced by Mahvash et al. [21]. A friction compensation algorithm was implemented for each compliant transmission joint of the da Vinci system. Hence, manipulation forces at the instrument tip could be estimated by the currents applied to the actuators with promising results. However, the compensator cancels only Coulomb friction when all friction surfaces of a considered joint move in the same direction, deteriorating the accuracy of the force feedback. Additionally, friction parameters are joint specific and can change by-and-by, which necessitates regular recalibration for each joint.

DLR Robot

This section describes in detail the medical robot developed at DLR. First, the requirements such as accuracy, manipulability, and payload as well as the optimization procedure to calculate the link lengths of the robot are given in the "Arm Design" section. Thereafter, the mechanical implementation is described in the "Robot Hardware" section.

Arm Design

Following the guideline of an ideal telemanipulator described in the "Requirements for an Ideal Telemanipulator" section, the

design objective of the DLR robot was to build a compact, kinematically redundant, intuitively operated robot arm for a wide range of medical applications. Besides the telemanipulated and classic preprogrammed operation, the robot shall also be suited for semiautonomy (e.g., some DoF are controlled by the surgeon, while the robotic system controls the remaining DoF optimally according to the task [22]). Investigation of possible applications (e.g., visceral surgery, cardiac surgery, orthopedics, urology, neurology) showed several fields with similar requirements. A generic robot arm tailored to these demands, can therefore cover different areas and thus reduce costs for robot-assisted surgery.

Mainly based on the experiences gained from the development of a light-weight robot [23], the DLR medical arm has 7 DoF as shown in Figure 2, and two additional DoF (Θ_8 and Θ_9) are added if an actuated instrument is used. With the loss of 2 DoF due to kinematic restrictions at the entry point into the human body, all 6 DoF remain for the manipulation of the instrument tip inside the patient, and 1 DoF outside the patient body enables nullspace motion. Except for the wrist joint Θ_7, the kinematic structure of the medical arm is anthropomorphic. The intersecting joints $\Theta_{1..3}$ form the shoulder, the elbow is actuated through joint $\Theta_{4,5}$, and the wrist consists of the joints $\Theta_{6,7}$. See Figure 2(a) for the kinematic structure of the medical arm in the Denavit-Hartenberg formalism [24]. Because of the intersection of the last three axes $\Theta_{5..7}$ and with joint Θ_2 or joint Θ_3 held constant, an analytic solution of the inverse kinematics is possible, thus providing a deterministic and fast method to calculate the necessary joint positions to adopt a given tool tip position. Additionally, to enable nullspace motion, kinematic redundancy allows in general for the reduction of the number of singular configurations [25]. The kinematic structure of the DLR robot contains only two singular configurations e_i inside the joint limits and allows for an analytic calculation [25]:

$$e_1: \quad \Theta_4 = 0^\circ, \quad \text{and} \quad e_2: \quad \Theta_5 = 90^\circ \wedge \Theta_6 = 0^\circ.$$

This a priori knowledge enables the use of computationally cheap strategies for singularity avoidance in analogy with well-known strategies for joint limit avoidance. Stability and safety of the system is thereby further increased.

The lengths of the segments l_1 and l_2 were determined during a design optimization, including a systematic analysis of the range of applications. Therefore, different workspaces were derived from the envisioned robot-assisted procedures on the ureter, gallbladder, and appendix, as well as from orthopedic operations and cardiac surgeries such as heart valve and bypass procedures. Both open and minimally invasive interventions were considered. Inside the workspaces, certain performance criteria as described later have to be met.

The required absolute positioning accuracy of the robot in combination with a navigation system was derived from the anatomic conditions for the placement of pedicle screws and is smaller than 1 mm for translation and 1° for rotation. The relative positioning accuracy of the robot end effector was determined by the accuracy demands of the bypass surgery and should be better than 0.1 mm for translation and 0.5° for rotation, respectively [26]. Furthermore, the robot end effector should be able to move with a speed of at least 60 mm/s and

The MMI should allow for an intuitive and ergonomic working style to relieve the surgeon from stress.

30°/s within selected target areas [26]. These values stem from the analysis of requirements for the robot-assisted compensation of stabilized heart movement in beating-heart surgery.

Assessment of performance requirements was possible by the definition of new manipulability and accuracy measures that include the motion constraint due to the entry point and provide a clear relation to the required performance parameters [27]. In case of the manipulation measure, the differential inverse kinematics are considered:

$$\dot{\Theta} = \mathbf{E}[\, v_x \quad v_y \quad v_z \,]^{\mathrm{T}} + \mathbf{F}[\, \omega_x \quad \omega_y \quad \omega_z \,]^{\mathrm{T}}, \qquad (1)$$

with

$$\mathbf{E}, \mathbf{F} \in \mathbb{R}^{9\times 3},$$

which relates the joint velocities $\dot{\Theta}$ to the translational respective rotational velocities $[v_i, \omega_i]$ at the tool tip. In (1), the motion restriction at the entry point is included as suggested in [28]: for each joint $i \in [1, \ldots, 9]$, the maximum occurring velocity $\dot{\Theta}_{i,\max}$ to perform a tool tip velocity $\dot{x}_{\min}$ and $\dot{\omega}_{\min}$ can

i	1	2	3	4	5	6	7
a_{i-1}	0	0	0	l_1	0	0	0
α_{i-1}	0	$-\frac{\pi}{2}$	$\frac{\pi}{2}$	$-\frac{\pi}{2}$	$\frac{\pi}{2}$	$-\frac{\pi}{2}$	$\frac{\pi}{2}$
d_i	d_1	0	0	0	l_2	0	d_7
θ_i	0	$-\frac{\pi}{2}$	0	$\frac{\pi}{2}$	0	0	0

(a)

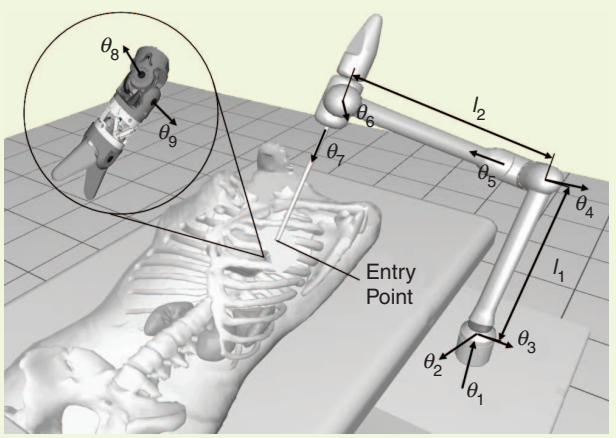

(b)

Figure 2. *Kinematic structure of the DLR medical robot with an actuated instrument for laparoscopic surgery.*

Telemanipulators are the key components in telesurgery systems, as they transfer the surgeon's commands to the patient's body.

be computed by solving an optimization problem and yields (see [29] for further details):

$$\dot{\Theta}_{i,\max} = \sqrt{e_{i1}^2 + e_{i2}^2 + e_{i3}^2}\ \dot{x}_{\min} + \sqrt{f_{i1}^2 + f_{i2}^2 + f_{i3}^2}\ \dot{\omega}_{\min},$$

where $[e_{ij}, f_{ij}]$ denotes the entries of $[\mathbf{E}, \mathbf{F}]$. The maximum joint velocity $\dot{\Theta}_{\max} = \max(\dot{\Theta}_{i,\max})$ serves as the manipulability measure. For a given, desired minimal velocity at the tool tip, a low value of $\dot{\Theta}_{\max}$ indicates low joint velocities, i.e., good manipulability. See [27] for details on the accuracy measure.

Moreover, criteria to assure the absence of collisions as well as high visibility and dexterity were integrated [30]. To achieve a slender and lightweight design, the optimization goal was to minimize the sum of the link lengths l_1 and l_2 (Figure 2) while observing all performance requirements throughout all workspaces. The formulated optimization problem was solved by means of genetic algorithms and resulted in $l_1 = 310$ mm and $l_2 = 385$ mm. The overall size of the DLR medical arm is thus close to the dimension of the human arm.

In contrast to many other surgical robots, the motion about the invariant insertion point is not guaranteed because of a dedicated mechanical design (e.g., da Vinci) but will be guaranteed by control algorithms. This is because we believe that an implementation of constraints by software means adds more flexibility to the system which is one of the design goals. However, it has been guaranteed that no laceration of the entry point due to programming errors or computer failure occurs. In medical applications

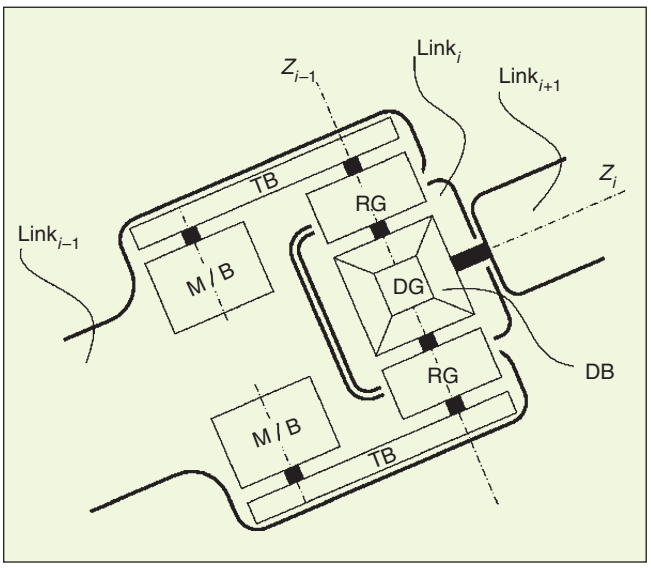

Figure 3. *Pitch-roll coupled joint.*

care has to be taken to obtain a fail safe system under all circumstances. This can be guaranteed by special measures including redundant (joint) measurement, redundant computation, dedicated software development process etc., which are also necessary for any kind of medical robots. Thus, the additional effort to implement a safe software-based solution to obtain an invariant point and to avoid injury of the patient is expected to be small.

To determine maximum necessary manipulation forces of the robot arm, drilling of holes for pedicle screw placement was taken as a medical reference application. Robot-assisted drilling tests on bovine spine (in vitro) were carried out to assess the maximum forces with respect to magnitude and distribution. A maximum robot payload of 30 N (worst case) was obtained [31].

Robot Hardware

The various medical setups in MIRS include up to four robots near the patient in an already crowded and hardly predictable OR environment. Because these systems move autonomously, the danger of robots colliding with each other and with the patient, personnel, or equipment is evident. The lack of predictability of the OR environment and the close interaction with nontechnical staff makes industrial solutions hardly suitable for the OR. Therefore, a central design issue with the DLR robot is a natural predictability of the system motion. Based on the optimized kinematics, a structure was designed that utilizes analogies with the human arm, serially structured into a 3-DoF shoulder joint, an upper arm, a 2-DoF elbow, a forearm, and a 2-DoF wrist (see the "Arm Design" section). The mechanical capabilities as well as the shape and the motion of the robot resemble those of the human arm. Further paradigms of the DLR robot arm are as follows: 1) low robot weight of less than 11 kg to simplify the setup or removal in an emergency situation, 2) slim design to reduce the required space, 3) joint redundancy to allow for an independent motion of the robot elbow from TCP motion (collision avoidance), 4) torque controllable joints for whole arm interaction and load surveillance, 5) backdrivable joints in case of a system breakdown, 6) absolute position sensors to minimize initialization procedures, and 7) skeletal structure with integrated electronics.

To form compact groups of joints with intersecting axis, 2-DoF coupled joints were designed. Coupled by a cardanic differential bevel gear, two motors equipped with safety brakes and reduction gears drive the joint. Supplemented with a single rotational first joint Θ_1, the robot shoulder consists of a pitch-yaw coupled joint ($\Theta_{2,3}$), whereas elbow ($\Theta_{4,5}$) and wrist ($\Theta_{6,7}$) are realized by pitch-roll coupled joints (see Figure 2 for the robot configuration).

As depicted in Figure 3, the motor brake assembly (M/B) axis has a parallel offset to the reduction gear (RG) axis, which is collinear to the joint pitch axis (Z_{i-1}). This offset is bridged by means of tooth belt (TB) drives. The two reduction gears are coupled by a differential bevel gear (DG) with the bevels pivoted in link i. If link $i+1$ is aligned to the axis of the driven bevel (DB) (Figure 3), a pitch-roll coupled joint is possible. By rotating the index position of link i by 90° about axis Z_{i-1} and by attaching link $i+1$ with the driven bevel gear (DB), a pitch-yaw configuration as used in joint unit ($\Theta_{2,3}$) of the

DLR robot is established. The coupled joint design offers many advantages: 1) both motors and brakes being on the same side of the joint unit, allowing for a reduction of electronic components, 2) compact joint dimensions, 3) intersecting axis, and 4) the use of redundant kinematics to optimize efficiency.

Optimizing efficiency needs further annotations. In a coupled joint as described above, the torque of the motors is added as given in (2), where τ_i are the joint torques and τ_{m_i} are the motor torques:

$$\begin{pmatrix} \tau_1 \\ \tau_2 \end{pmatrix} = \frac{1}{2} \begin{bmatrix} 1 & 1 \\ -1 & 1 \end{bmatrix} \begin{pmatrix} \tau_{m_1} \\ \tau_{m_2} \end{pmatrix}. \quad (2)$$

The second joint torque is formed by the sum of both motor torques if one joint torque is zero. Maximum payload capacity is not required in every kinematic posture. It is reasonable to use adequate kinematic postures of the redundant robot arm in high payload applications. In the case of a robot with coupled joints, a posture that creates mostly single axis loads on the coupled joints offers the opportunity of the addition of motor torques as shown earlier. As a result of the joint groups realized by coupled joints, upper arm and forearm can be used to integrate the electronics for the elbow and the wrist joints, respectively (Figure 4).

The robot is connected to an external control computer via fiber optics, which ensures galvanic decoupling of the equipment and thus the reduction of patient leakage currents. Current control of the robot motors is carried out locally within the joint digital electronics, (Figure 4). The controller is implemented on field programmable gate arrays (FPGAs), which are also responsible for the communication between the joint units and the external control computer as well as for the joint unit house keeping. The FPGAs are interlinked with a slim, package-based protocol (HIC, IEEE 1355). Based on the physical Multi-Gigabit-Transceiver of the FPGAs and by the implementation of the higher layers of the SpaceWire (ECSS-E50-12) protocol in the FPGA, a very flexible communication infrastructure with a bandwidth of 1 Gb/s and cycle time less than 333 μs was achieved (see [22] for details).

The joint state control for the coupled joints as well as the Cartesian controller run on the external control computer. These state control laws allow for a sensitive impedance control of the joints as well as for stiff position control. In combination with the joint torque sensor, they also allow for a direct haptic interaction with the robot by the OR personnel and for collision detection. For details on the control laws, see [32] and [33].

DLR Instruments

In this section, the surgical instruments that can be attached to the robot are presented. This includes the mechanical design of two additional DoF at the instrument tip to regain full manipulability in MIS, an actuated functional end, and the drive box necessary to actuate them. Thereafter, a miniaturized force-torque sensor that can be placed near the distal end of the instrument to measure contact forces is described. Such a sensor is a prerequisite for a variety of advanced features including force control, force feedback, and autonomy.

The lack of predictability of the OR environment and close interaction with nontechnical staff makes industrial solutions hardly suitable for the OR.

Mechanical Design

Along with the DLR robotic surgery system, a minimally invasive instrument was designed and prototyped. It combines a 6-DoF force-torque sensor with a 2-DoF cable driven joint and all necessary mechatronic components in one self-contained unit (Figure 5).

The additional DoF required to achieve full dexterity inside the patient are provided by a cardanic (universal) joint (Figure 6). The range of motion in the joint is restricted to about ±40° in both directions, caused by an inherent limitation of universal joints. The setup of the drive cables in the joint makes the cables run tangential to the drive pulleys at all times. Therefore, the lengths of both cable loops remain constant for every joint position. The middle of each cable loop is tied to the distal component of the joint, while the proximal ends are

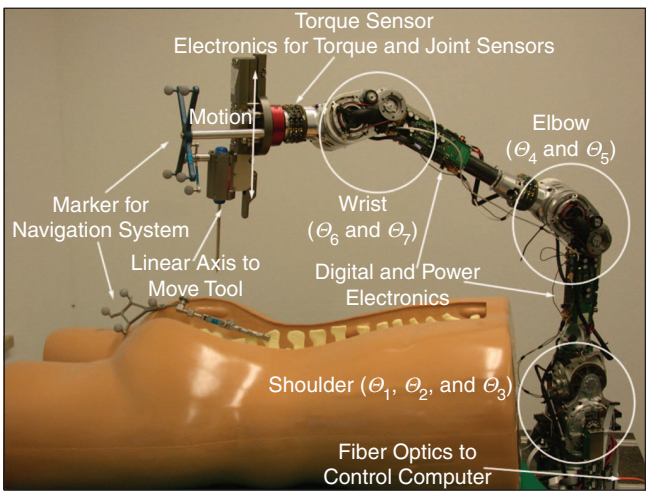

Figure 4. *New medical robot in a navigated spine surgery application.*

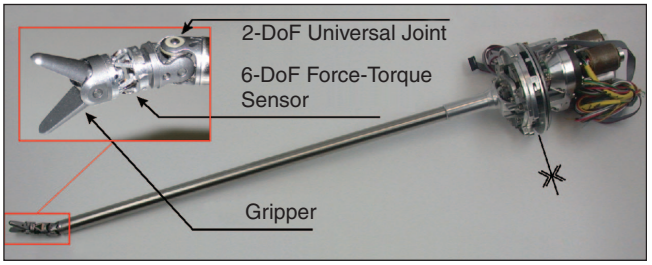

Figure 5. *Photo of the entire, prototypic minimally invasive instrument. The functional end is heightened, and the separation plane for sterilization purposes is marked.*

High dynamics of the robot make it suitable for advanced tasks, such as motion compensation for procedures on the beating heart.

connected crosswise at the actuators. With this layout, only two fixed rotary drives are needed to fully actuate the joint, yielding linear transmission characteristics. Driving only one actuator results in a tilting motion of the instrument tip at a 45° angle to the principal axes of the joint:

$$\theta_8 = \frac{r_M}{2r_a}(\beta - \alpha) \quad \text{and} \quad \theta_9 = \frac{r_M}{2r_a}(\beta + \alpha), \tag{3}$$

where r_M is the radius of motor pulley, r_a is the radius of joint pulley (3 mm), α, β are the actuator positions, and θ_8, θ_9 are joint angles.

Maximum cable force for the joint actuation is 100 N. This results in manipulation forces of 20 N at the instrument tip, with the gripping force being 20 N [17]. The gripper is actuated by one cable counteracted by a spring. The cable force necessary to close the gripper and securely hold a needle is estimated to be 70 N.

The instrument components are too complex and expensive for a disposable design. For repeated, cost-effective use, the components with patient contact have to be sterilizable, i.e., by autoclaving as a standardized process. Therefore, the drive unit was designed to be separable into two reconnectable components (Figure 5): one autoclavable section in contact with the patient without any thermally instable components and one spray-sanitized section not in contact with the patient containing motors and electronics. The drive unit itself is located at the distal end of the surgical manipulator arm described earlier and at the proximal end of the 10 mm diameter instrument shaft.

Force Sensor

To obtain realistic force information, a sensor is preferably placed close to the instrument tip, minimizing the errors due to friction between the instrument and the point of incision.

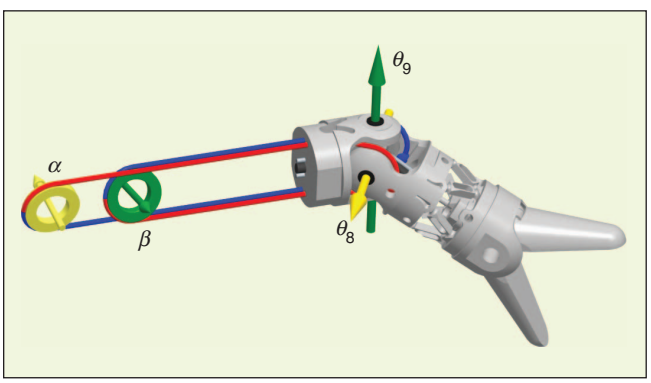

Figure 6. *Prototypic functional end of the MIS instrument with the layout of the drive cables.*

The sensor should be decoupled from the drive mechanism to prevent the influence of driving forces, backlash, and friction on the sensor's performance [3]. A placement between the gripper and joint was selected, as the sensor is only subjected to the gripper actuation force at this location. It is not influenced by the joint actuation forces as in placements proximal to the joint. The gripper actuation force, also acting on the sensor, is measured for the calculation of the gripping force. Therefore, the force-torque sensor output can be compensated for this parasitic load simultaneously. However, the electrical connections to the sensor have to be routed through the joint, requiring highly flexible, isolated, multistrand wires. This location requires the sensor to be of roughly cylindrical shape, with a preferably central hollow section to accommodate for the gripper drive cable and mechanics.

A Stewart Platform-based force-torque sensor was chosen for its high stiffness, adaptable properties, annular shape, and scalability. Furthermore, only longitudinal force transducers are required,which facilitates the future application of force transducers other than resistive strain gauges. Analysis and properties of Stewart Platform transducers were presented previously by Sorli et al. [34], who outlined a set of variables ($R, L, \alpha, \beta, \gamma$, shown in Figure 7) sufficiently describing the geometry and thus the properties of the sensor. The characteristic matrix $\mathbf{A} \in \mathbb{R}^{6\times 6}$ describing the transformation of link forces to externally applied loads

$$[F_x, F_y, F_z, M_x, M_y, M_z]^T = \mathbf{A} \cdot [F_1, F_2, F_3, F_4, F_5, F_6]^T$$

is calculated using the method described by Sorli et al., where

$$\mathbf{A} = -\frac{1}{2} \cdot \begin{bmatrix} -2n & 2n & \sqrt{3}m+n & \sqrt{3}m-n & -\sqrt{3}m+n & -\sqrt{3}m-n \\ -2m & -2m & m-\sqrt{3}n & m+\sqrt{3}n & m+\sqrt{3}n & m-\sqrt{3}n \\ -2q & -2q & -2q & -2q & -2q & -2q \\ 2aq & 2aq & -aq & -aq & -aq & -aq \\ 0 & 0 & aq\sqrt{3} & aq\sqrt{3} & -aq\sqrt{3} & -aq\sqrt{3} \\ -2an & 2an & -2an & 2an & -2an & 2an \end{bmatrix},$$

with

$$m = \cos(\alpha)\cos(\beta)$$
$$n = \cos(\alpha)\sin(\beta)$$
$$q = \sin(\alpha).$$

To find a sensor geometry that is well conditioned and optimized for the force range expected in a surgical application, the following search method is used. The radius of the base R and the link length L are determined by the space available in the instrument. Geometrically valid combinations (nonintersecting links) of $R, L, \alpha, \beta, \gamma$ are used to calculate $\mathbf{A}$. Various sets of maximally expected external loads $[F_x, F_y, F_z, M_x, M_y, M_z]^T$ are selected. These sets must contain at least one load in each of the six principal directions.

Every member of the external load set is premultiplied by $\mathbf{A}^{-1}$, yielding the corresponding set of internal leg forces $\mathbf{J} = [F_1, F_2, F_3, F_4, F_5, F_6]^T$. The conditioning number of the internal leg force set is a measure of the isotropy of the sensor structure with respect to the external load set. This however is not an isotropy in the classical definition, since the external loads in the principal directions need not be equal.

For the load set $F_{x,y,z} = 10\,\text{N}$, $M_{x,y} = 150\,\text{Nmm}$, $M_z = 100\,\text{Nmm}$, the following parameters were selected as optimal sensor geometry: $R = 4.2\,\text{mm}$, $L = 3.9\,\text{mm}$, $\alpha = 65°$, $\beta = 90°$, $\gamma = 36°$, yielding a conditioning number of 6.3 and a joint separation of $i = 1.1\,\text{mm}$.

For a sensor of less than 10 mm diameter, ball or universal joints normally used in Stewart Platforms are not suitable because of their high complexity of manufacturing and assembly. These are replaced by flexural joints creating a monolithic sensor structure as shown in Figure 8. Given appropriate design of flexural hinges and leg cross section, the results of an FEM analysis are in very good agreement with the prediction by the ideal analytical model [3]. Figure 8 shows the simulated surface strain for an external load of 30 N. Generally, the cross section of the flexural hinges should be as small as possible to avoid parasitic bending moments from being created in the legs. However, plastic deformation and, therefore, hysteresis will first occur at the point of highest stress. To guarantee a high load capability, the cross-sectional areas of both hinge and leg should be roughly equal. Also, the location of the neutral fiber for bending of both the leg and hinge cross sections should be identical.

After fabrication and assembly of the strain gauges, the sensor is calibrated using a set of known weights applied in the six principal directions. The sensor is subjected to at least one complete loading and unloading cycle to determine the amount of hysteresis. Results of the calibration for one sensor are shown in Figure 9, with output values for all six load directions being shown in each graph. Output values for the load direction corresponding to the applied external load show an approximately linear unity response, whereas outputs for all other load directions are expected to remain zero.

The instrument presented here serves as a technology demonstrator and lab prototype, so the relatively large diameter of 10 mm is acceptable. Maintaining the proposed design of joint and sensor, a further reduction in diameter to about 7 mm is possible using established manufacturing and assembly techniques. However, with the drawback of reducing the load capability of the entire instrument to about 50% of the current specifications.

Conclusions and Outlook

In this article, a new fully torque-controlled, light-weight, and kinematically redundant robot for both open and laparoscopic surgery is presented. This robot meets the requirements for medical robots summarized in the "Requirements for an Ideal Telemanipulator" section. Because of its kinematic redundancy the robot configuration can easily be reconfigured without changing the TCP pose. This allows for a flexible OR setup and reduces the risk of collisions. Using joint torque sensors and the impedance control laws, this can be achieved by haptic interaction. The light-weight and slender robot can be mounted or unmounted by one person, and thus the flexibility in the OR is increased. High dynamics of the robot make it

Because of its kinematic redundancy, the robot configuration can easily be reconfigured without changing the TCP pose.

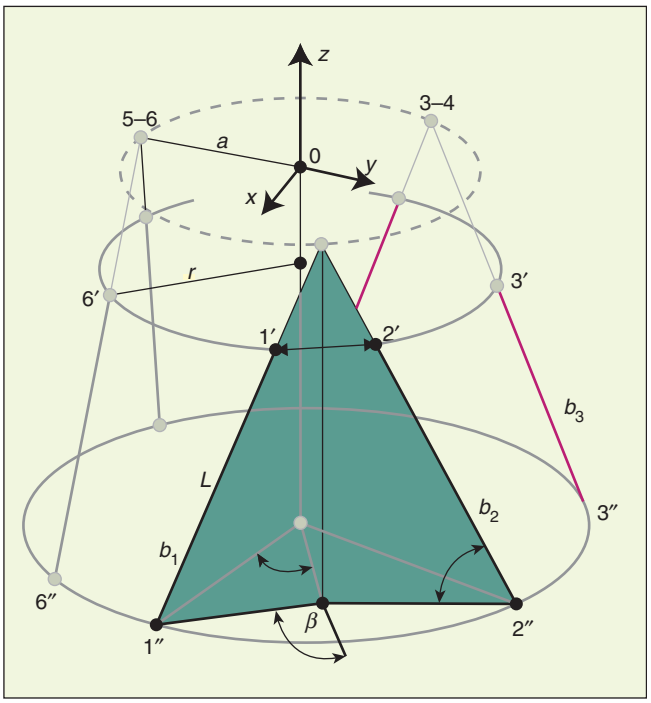

Figure 7. *Geometrical parameters of Stewart Platform: base radius R and platform radius r.*

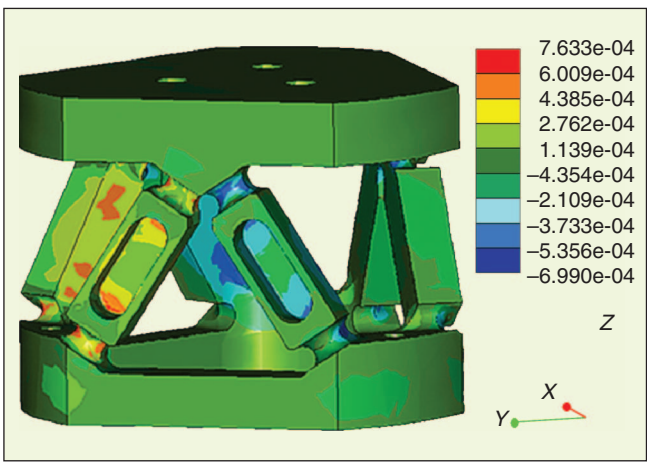

Figure 8. *Average strain on force-torque sensor for load $F_y = 30\,\text{N}$.*

Sensorized and actuated instruments enable the surgeon to regain access to manipulation forces.

suitable for advanced tasks, such as motion compensation for procedures on the beating heart.

Sensorized and actuated instruments as presented in the "DLR Instruments" section enable the surgeon to regain access to manipulation forces. Thus, it is likely that the risk of unintentional damage to suturing material and delicate tissue can be reduced. Furthermore, force control of the instrument is possible and intelligent assistance functions (e.g., intelligent holder, following the organ motion automatically) can be implemented. Actuated instruments reestablish full dexterity inside the patient and are a prerequisite for correct hand eye-coordination as experienced in open surgery.

The described components, robot and sensorized instrument, were separately built and successfully tested [35]. A first complete telepresence setup was realized with three robots. Two are carrying MIS instruments as described earlier. One additional robot is carrying a standard endoscopic stereo camera. The teleoperator console consists of two commercially available haptic devices (omega.7, Force Dimension, Inc., Switzerland) and an autostereoscopic display. The haptic input devices provide 7 DoF, of which four are active (translations and gripper). The teleoperation controller is a Cartesian position-force controller, with positions being sent from the master to the slave and forces sent back from the slave to the master. The local controller for the telemanipulator is implemented with a 9-DoF inverse kinematics that takes respect of the trocar point and a multiple-input and multiple-output (MIMO) position controller in joint space [36]. The surgeon can also use the haptic input devices to move the endoscopic camera in an intuitive way. This setup is the basis for further research and investigation including the role of force feedback.

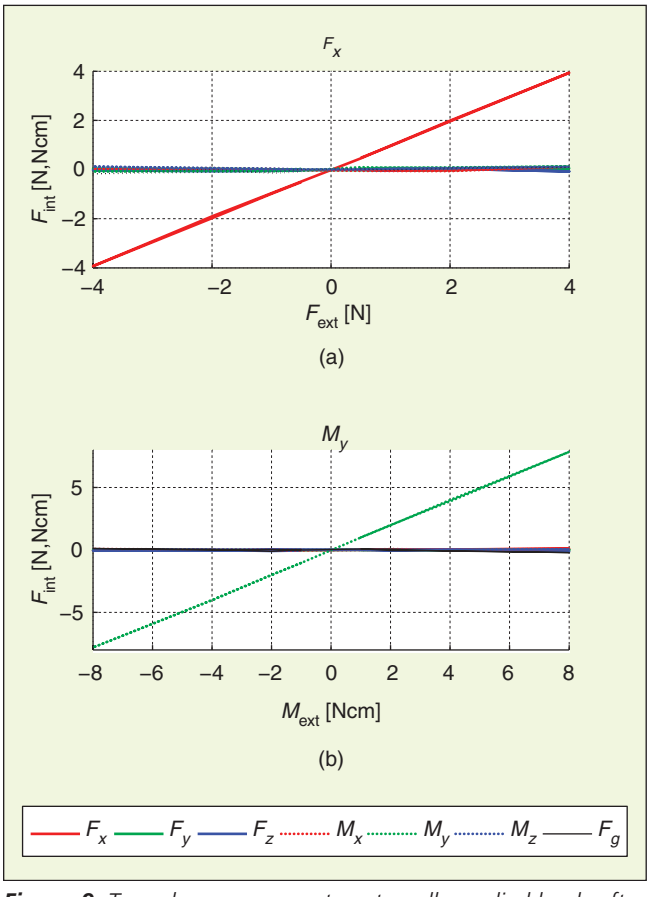

Figure 9. *Transducer response to externally applied loads after calibration. Shown are exemplary results for (a) F_x and (b) M_y. Results for the other directions show similar behavior.*

Autonomous functions to support the surgeon may be introduced into the OR in the near future. These functions relieve the surgeon of repetitive and tiring tasks and increase the surgeon's situational awareness. They may include motion compensation [4], [37] and automatic camera guidance [6].

On the horizon, interesting new challenges arise. The natural orifice transluminal endoscopic surgery (NOTES) technology, which is promoted, e.g., by Natural Orifice Surgery Consortium for Assessment and Research (NOSCAR), will allow for surgery with long flexible instruments being inserted through natural body orifices. Thus, no visible scars occur. The white paper of NOSCAR gives a brief introduction and provides further details [38]. For first experimental animal trials, see [39], which describes a novel access to the peritoneal cavity through the anus.

Acknowledgments

We gratefully acknowledge the financial support by the German Research Foundation (DFG) as this project was funded within the Collaborative Research Center SFB 453 "High-Fidelity Telepresence and Teleaction." Additionally, we thank the company BrainLAB and the Bavarian Research Foundation (BFS) for substantial funding of the robot described in this article.

Keywords

Medical robotics, minimally invasive robotic surgery, force feedback, telemanipulation, robot development.

References

[1] M. R. Treat, "A surgeon's perspective on the difficulties of laparoscopic surgery," in *Computer-Integrated Surgey*, R. H. Taylor, S. Lavallee, G. Burdea, and R. Mosges, Eds. Cambridge, MA: MIT Press, 1995, pp. 559–560.

[2] M. Helmy, "A comparative study between laparoscopic versus open appendectomy in men," *J. Egypt Soc. Parasitol.*, vol. 31, no. 2, pp. 555–562, Aug. 2001.

[3] B. Kuebler, U. Seibold, and G. Hirzinger, "Development of actuated and sensor integrated forceps for minimally invasive robotic surgey," *Int. J. Med. Robot*, vol. 1, no. 3, pp. 96–107, Sept. 2005.

[4] T. Ortmaier, *Motion Compensation in Minimally Invasive Robotic Surgey.* Berlin, Germany: Springer-Verlag, 2003.

[5] Y. Nakamura, "Virtual stillness and small size robot system that occupies less space in OR," presented at the Int. Conf. Robotics, Workshop on

Recent Advances in Medical Robotics and Automation (ICRA), Taipei, Taiwan, 2003.

[6] G.-Q. Wei, K. Arbter, and G. Hirzinger, "Real-time visual servoing for laparoscopic surgery," *IEEE Eng. Med. Biol.*, vol. 16, no. 1, pp. 40–45, Jan./Feb. 1997.

[7] M. Jakopec, S. Harris, F. Y. Baena, P. Gomes, J. Cobb, and B. Davies, "Preliminary results of an early clinical experience with the Acrobot system for total knee replacement surgery," in *Proc. 5th Int. Conf. Medical Image Computing and Computer-Assisted Intervention (MICCAI)*, Tokyo, Japan, Sept. 2002, vol. 2488, pp. 256–263.

[8] V. Falk, S. Jacobs, J. Gummert, and T. Walther, "Robotic coronary artery bypass grafting (CABG)—the Leipzig experience," *Surg. Clin. North. Am.*, vol. 83, no. 6, pp. 1381–1386, Dec. 2003.

[9] S. Jacobs, D. Holzhey, B. Kiaii, J. Onnasch, T. Walther, F. Mohr, and V. Falk, "Limitations for manual and telemanipulator-assisted motion tracking: Implications for endoscopic beating-heart surgery," *Ann. Thorac. Surg.*, vol. 76, no. 6, pp. 2029–2036, 2003.

[10] D. A. Lawrence, "Stability and transparency in bilateral teleoperation," *IEEE Trans. Robot. Automat.*, vol. 9, no. 5, pp. 624–637, Oct. 1993.

[11] R. H. Taylor and D. Stoianovici, "Medical robotics in computer-integrated surgery," *IEEE Trans. Robot. Automat.*, vol. 19, no. 5, pp. 765–781, 2003.

[12] J. M. Sackier and Y. Wang, "Robotically assisted laparoscopic surgery: From concept to development," in *Computer-Integrated Surgery*, R. H. Taylor, S. Lavallee, G. Burdea, and R. Mosges, Eds. Cambridge, MA: MIT Press, 1995, pp. 577–580.

[13] G. Guthart and J. Salisbury, "The intuitive telesurgery system: Overview and application," in *Proc. IEEE Int. Conf. Robotics and Automation (ICRA)*, San Francisco, CA, Apr. 2000, pp. 618–621.

[14] T. Hu, A. Castellanos, G. Tholey, and J. Desai, "Real-time haptic feedback in laparoscopic tools for use in gastro-intestinal surgery," in *Proc. Medical Image Computing and Computer-Assisted Intervention—MICCAI 2002: 5th Int. Conf.*, Tokyo, Japan, Sept. 2002, pp. 66–74.

[15] N. Zemiti, T. Ortmaier, M.-A. Vitrani, and G. Morel, "A force controlled laparoscopic surgical robot without distal force sensing," in *Proc. ISER 2004; 9th Int. Symp. Experimental Robotics*, Singapore, June 2004, pp. 153–163.

[16] S. Shimachi, S. Hirunyanitiwatna, Y. Fujiwara, A. Hashimoto, and Y. Hakozaki, "Adapter for contact force sensing of the da Vinci robot," *Int. J. Med. Robot.*, vol. 4, no. 2, pp. 121–130, June 2008.

[17] U. Seibold, B. Kübler, and G. Hirzinger, "Prototype of instrument for minimally invasive surgery with 6-axis force sensing capability," in *Proc. IEEE Int. Conf. on Robotics and Automation (ICRA)*, Barcelona, Spain, Apr. 2005, pp. 498–503.

[18] T. Ortmaier, B. Deml, B. Kübler, G. Passig, D. Reintsema, and U. Seibold, Robot assisted force feedback surgery in *Advances in Telerobotics* (Springer Tracts in Advanced Robotics) M. Ferre, M. Buss, R. Aracil, C. Melchiorri, and C. Balaguer, Eds. Berlin, Germany: Springer-Verlag, 2007, pp. 361–379.

[19] C. Wagner, N. Stylopoulos, and R. Howe, "The role of force feedback in surgery: Analysis of blunt dissection," in *Proc. 10th Ann. Haptics Symp.*, Pisa, Italy, Mar. 2002, pp. 68–74.

[20] Y. Kobayashi, S. Chiyoda, K. Watabe, M. Okada, and Y. Nakamura, "Small occupancy robotic mechanisms for endoscopic surgery," in *Proc. Medical Image Computing and Computer-Assisted Intervention–MICCAI 2002: 5th Int. Conf.*, vol. 2488/2002, Berlin, Germany: Springer-Verlag, 2002, pp. 75–82.

[21] M. Mahvash, J. Gwilliam, R. Agarwal, B. Vagvolgyi, L.-M Su, D. Yuh, and A. Okamura, "Force-feedback surgical teleoperator: Controller design and palpation experiments," in *Proc. Symp. Haptic Interfaces for Virtual Environment and Teleoperator Systems (Haptics 2008)*, Mar. 2008, pp. 465–471.

[22] T. Ortmaier, H. Weiss, U. Hagn, M. Grebenstein, M. Nickl, A. Albu-Schäffer, Ch. Ott, S. Jörg, R. Konietschke, L. Le-Tien, and G. Hirzinger, "A hands-on-robot for accurate placement of pedicle screws," in *Proc. IEEE Int. Conf. on Robotics and Automation (ICRA)*, Orlando, Florida, May 2006, pp. 4179–4186.

[23] G. Hirzinger, A. Albu-Schäffer, M. Hähnle, I. Schaefer, and N. Sporer, "On a new generation of torque controlled light-weight robots," in *Proc. 2001 IEEE Int. Conf. Robotics and Automation*, Seoul, Korea, May 2001, pp. 3356–3363.

[24] J. J. Craig, *Introduction to Robotics*. Reading, MA: Addison-Wesley, 1989.

[25] R. Konietschke, G. Kirzinger, and Y. Yan, "All singularities of the 9-DoF DLR medical robot setup for minimally invasive applications," in *Advances in Robot Kinematics*, J. Lenarcic and B. Roth, Eds. Berlin, Germany: Springer-Verlag, 2006, pp. 193–200.

[26] R. Konietschke, T. Ortmaier, H. Weiß, R. Engelke, and G. Hirzinger, Optimal design of a medical robot for minimally invasive surgery, presented at Jahrestagung der Deutschen Gesellschaft für Computer und Roboterassistierte Chirurgie (CURAC), Nümberg, Germay, pp. 4–7 Nov. 2003 [Online]. Available: http://www.robotic.dlr.de/koniets/publications

[27] R. Konietschke, T. Ortmaier, H. Weiss, and G. Hirzinger, "Manipulability and accuracy measures for a medical robot in minimally invasive surgery," in *On Advances in Robot Kinematics*, J. Lenarcic and C. Galletti, Eds. The Netherlands: Kluwer Academic, 2004, pp. 191–198.

[28] T. Ortmaier and G. Hirzinger, "Cartesian control of robots with working-position dependent dynamics," in *Proc. 6th Int. IFAC Symp. Robot Control (SYROCO 2000)*, vol. 2, Vienna, Austria, Sept. 2000, pp. 717–721.

[29] R. Konietschke, "Aufbauoptimierung für Roboter in medizinischen Anwendungen," Diploma Thesis, Munich Univ. of Technology, Germany, 2001 [Online]. Available: http://www.robotic.dlr.de/koniets/publications

[30] R. Konietschke, T. Ortmaier, U. Hagn, G. Hirzinger, and S. Frumento, "Kinematic design optimization of an actuated carrier for the DLR multi-arm surgical system," in *Proc. 2006 IEEE/RSJ Int. Conf. on Intelligent Robots and Systems (IROS)*, Beijing, China, Oct. 2006, pp. 4381–4387.

[31] T. Ortmaier, H. Weiss, C. Ott, G. Hirzinger, and G. Schreiber, "A soft robotics approach for navigated pedicle screw placement—First experimental results," in *Proc. 2006 Computer Assisted Radiology and Surgery (CARS), 20th Int. Congr. and Exhibition*, Osaka, Japan, 28 June–1 July 2006.

[32] C. Ott, A. Albu-Schäffer, A. Kugi, S. Stramigioli, and G. Hirzinger, "A passivity based Cartesian impedance controller, Part I: Torque feedback and gravity compensation," in *Proc. 2004 IEEE Int. Conf. on Robotics and Automation*, pp. 2659–2665.

[33] A. Albu-Schäffer, C. Ott, and G. Hirzinger, "A passivity based Cartesian impedance controller—part II: Full state feedback, impedance design and experiments," in *Proc. 2004 IEEE Int. Conf. on Robotics and Automation*, pp. 2666–2672.

[34] M. Sorli and S. Pastorelli, "Six-axis reticulated structure force/torque sensor with adaptable performances," *Mechatronics*, vol. 5, no. 6, pp. 585–601, 1995.

[35] U. A. Hagn, M. Nickl, S. Jörg, G. Passig, T. Bahls, A. Nothhelfer, F. Hacker, L. Le-Tien, A. Albu-Schäffer, R. Konietschke, M. Grebenstein, R. Warpup, R. Haslinger, M. Frommberger, and G. Hirzinger, "The DLR MIRO—A versatile lightweight robot for surgical applications," *Int. J. Ind. Robot.*, vol. 35, no. 4, pp. 324–336, Aug. 2008.

[36] L. Le-Tien, A. Albu-Schäffer, and G. Hirzinger, "MIMO state feedback controller for a flexible joint robot with strong joint coupling," in *Proc. IEEE Int. Conf. on Robotics and Automation (ICRA)*, Rome, Italy, Apr. 2007, pp. 3824–3830.

[37] R. Ginhoux, J. Gangloff, M. deMathelin, L. Soler, M. A. Sanchez, and J. Marescaux, "Beating heart tracking in robotic surgery using 500 Hz visual servoing, model predictive control and an adaptive observer," in *IEEE Int. Conf. on Robotics and Automation (ICRA)*, New Orleans, LA, Apr. 2004, pp. 274–279.

[38] D. Rattner and A. Kalloo, "ASGE/SAGES Working Group on Natural Orifice Transluminal Endoscopic Surgery," *Gastrointest. Endosc.*, vol. 63, no. 2, pp. 199–203, 2006.

[39] D. Wilhelm, A. Meining, S. von Delius, A. Fiolka, S. Can, C. H. von Weyhern, A. Schneider, and H. Feussner, "An innovative, safe and sterile sigmoid access (ISSA) for NOTES," *Endoscopy*, vol. 39, no. 5, pp. 401–406, 2007.

Ulrich Hagn received his Dipl.-Ing. degree in mechanical engineering from the Technical University of Munich in 1998. Since then, he has been working at the Institute of Robotics and Mechatronics, German Aerospace Center (DLR), in the field of medical robotics and laser range sensors. He has participated in several national and international projects, including AccuRobas, SKILLS, SFB-453, Naviped, and Mirosurge. Since 2002, he has been leading the development of light weight robots for surgical applications at the DLR.

Tobias Ortmaier received his Dipl.-Ing. degree in electrical engineering and information technology and his Dr.-Ing. degree from the Technical University of Munich, Germany, in 1998 and 2003, respectively. From 1998 to 2008, he was a researcher at the Institute of Robotics and Mechatronics, DLR, working in the area of medical robotics, control, and computer vision. From 2003 to 2004, he worked as a postdoctoral fellow at the Laboratoire de Robotique de Paris, Univerité de Pierre et Marie Curie, France. From 2006 to 2008, he worked as a project manager for medical robotics research projects at the R&D department of KUKA Roboter GmbH in Augsburg, Germany. Since October 2008, he has been a full professor at the Institute of Robotics at the Leibniz University of Hanover, Germany.

Rainer Konietschke received his Dipl.-Ing. degree in mechanical engineering from the Technical University of Munich in 2002 and his master's degree from the École Centrale Paris. Since then, he has been working at the Institute of Robotics and Mechatronics, DLR, in the field of medical robotics, kinematics, optimization, and optimal surgery planning. He received his Ph.D. degree in electrical engineering from the Technical University of Munich in 2007. He has participated in several national and international projects, including AccuRobAs, SFB-453, Naviped, and Mirosurge.

Bernhard Kübler received his Dipl.-Ing. (FH) degree in biomedical engineering from the University of Applied Sciences Furtwangen, Germany, in 2000 and his Dipl.-Ing. degree in mechanical engineering from the University of Stuttgart, Germany, in 2003. Since then, he has been working as a research engineer at the Institute of Robotics and Mechatronics, DLR, in the field of medical robotics and MIRS instrument development. He participated in several national and international projects, including ASTMA, SFB-453, and Mirosurge.

Ulrich Seibold received his Dipl.-Ing. degree in mechanical engineering from the Technical University in Braunschweig in 1999. Since then, he is working at the Institute of Robotics and Mechatronics, DLR, in the field of medical instruments and force-torque-sensors. His main research interest is the miniaturization of electromechanical components and haptic feedback for surgical robotics.

Andreas Tobergte received his Dipl.-Inf. degree in computer engineering from the University of Mannheim in 2005, where he worked on the control of a medical robot. Since 2006, he has been working as a research engineer at the Institute of Robotics and Mechatronics, DLR, in the field of medical robotics and telepresence. He has participated in several national and international projects, including AccuRobas, SKILLS, SFB-453, and Mirosurge.

Mathias Nickl received his Dipl-Ing.(FH) degree in electrical engineering from the University of Applied Sciences Munich in 1998. Since then, he has been working at the Institute of Robotics and Mechatronics, DLR, as electronic system designer. His main interests are HW/SW-Codesign, model-driven design of complex mechatronic systems, and real-time signal-processing architectures.

Stefan Jörg received his Dipl-Ing.(FH) degree in electrical engineering from the University of Applied Sciences Kempten in 1995. Since then, he has been working at the Institute of Robotics and Mechatronics, DLR, in the fields of robotic vision and real-time signal processing architectures. His main interests are HW/SW-Codesign and model-driven design of complex mechatronic systems.

Gerd Hirzinger received his Dipl.-Ing. degree and doctoral degree from the Technical University of Munich in 1969 and 1974, respectively. Since 1969, he has worked at the Institute of Robotics and Mechatronics, DLR. In 1976, he became the head of the automation and robotics laboratory and in 1992 the director of the Institute of Robotics and Mechatronics at the DLR. In 1991, he received a joint professorship from the Technical University of Munich and in 2003 a honorary professorship at the Harbin Institute of Technology in China. He also received many national and international awards, e.g., Joseph-Engelberger Award in 1994, Leibniz-Award in 1995, JARA Award in 1995, Karl-Heinz-Beckurts Award in 1996, IEEE-Fellow Award in 1997, IEEE Pioneer Award of the Robotics and Automation Society in 2005, IEEE Field Award "Robotics and Automation" in 2007, and Nichols Medal of the International Federation of Automatic Control (IFAC) in 2008.

Address for Correspondence: Ulrich Hagn, Institute of Robotics and Mechatronics, German Aerospace Centre, Oberpfaffenhofen, 82234 Wessling, Germay. E-mail: Ulrich.hagn@dlr.de.